



# Detrital input and early diagenesis in sediments from Lake Baikal revealed by rock magnetism

François Demory<sup>a,\*</sup>, Hedi Oberhänsli<sup>a</sup>, Norbert R. Nowaczyk<sup>a</sup>, Matthias Gottschalk<sup>b</sup>,  
Richard Wirth<sup>b</sup>, Rudolf Naumann<sup>c</sup>

<sup>a</sup>Section 3.3, Climate Dynamics and Sediments, GeoForschungsZentrum, Telegrafenberg, 14473 Potsdam, Germany

<sup>b</sup>Section 4.1, Experimental Petrology and Geochemistry, GeoForschungsZentrum, Telegrafenberg, 14473 Potsdam, Germany

<sup>c</sup>Section 4.2, Inorganic and Isotope Geochemistry, GeoForschungsZentrum, Telegrafenberg, 14473 Potsdam, Germany

## Abstract

A rock magnetic study was performed on sediment cores from six locations in Lake Baikal. For a comprehensive approach of the processes influencing the rock magnetic signal, additional data are presented such as total organic carbon (TOC), total sulphur (TS), opal, water content and relative variations in iron and titanium measured on selected intervals. In glacial sediments, the magnetic signal is dominated by magnetite, which is considered to be of detrital origin. This predominance of magnetite is interrupted by distinct horizons of authigenic greigite, probably confined to reductive microenvironments. In interglacial stages, besides dilution by biogenic silica and a decreasing detrital input, the weakness of the rock magnetic signal is also due to a reductive dissolution of magnetic particles. The magnetic assemblage is strongly linked to the redox history of interglacial sediment. In the oxidised bottom sediments of Lake Baikal, a biogenic magnetite is observed [Peck, J.A., King, J.W., 1996. Magnetofossils in the sediments of lake Baikal, Siberia. *Earth Planet. Sci. Lett.* 140 (1–4), 159–172]. After burial under the redox front, the magnetite is preferentially dissolved, and detrital hematite remains dominant when the sedimentation rate is low and when the residence time of the magnetite close to the redox boundary is long. During these low sedimentation rate conditions, the redox front is preserved [Granina, L., Müller, B. and Wehrli, B., 2004. Origin and dynamics of Fe and Mn sedimentary layers in Lake Baikal. *Chem. Geol.* 205 (1–2), 55–72]. At constant sedimentation rate and fast burial, the magnetite is preserved or transformed into greigite when sulphate-reducing conditions are reached in the sediment. In interglacial sediments, the magnetic assemblages depict changes in the sedimentation rate, which are traced using the ratio of magnetite over hematite (S-ratio). At the beginning of interglacials, the sedimentation rate is constant with an assemblage magnetite+greigite (high S-ratio), and at the end of some interglacials, the sedimentation rate decreases with a predominance of hematite (low S-ratio).

© 2004 Elsevier B.V. All rights reserved.

**Keywords:** Lake Baikal; Late Quaternary; Rock magnetism; Diagenesis; Detrital input

\* Corresponding author. Present address. Centre Sed-Pal, FRE 2761, Université de Provence, place Victor Hugo, 13331 Marseille Cedex 03, France. Fax: +33 4 91 10 85 23.

*E-mail address:* [demory@up.univ-mrs.fr](mailto:demory@up.univ-mrs.fr) (F. Demory).

## 1. Introduction

Using rock magnetism, we can reconstruct the entire depositional history of magnetic particles in lake sediments. The magnetic minerals assemblage in lake sediments is first of all influenced by weathering and transport processes occurring in the catchment areas. After deposition, magnetic minerals can be altered, depending on chemical and biogenic processes occurring at the water/sediment interface and during diagenesis (e.g., Verosub, 1977; Snowball, 1993). In addition, during laboratory storage of the cores, the magnetic signal may also be altered (Thompson et al., 1980; Hilton, 1987). If diagenetic features such as dissolution and neoformation of magnetic particles can be identified and ruled out, rock magnetic properties become a powerful tool for tracing climate dynamics (e.g., Thouveny et al., 1994).

Since Lake Baikal sedimentation sensitively traces climate changes (Colman et al., 1995), it has been a natural laboratory for rock magnetic studies. However, rock magnetism was mainly used as a correlation tool since the concentration of magnetic minerals reflects the lithological variations in the sediment (e.g., Sakai et al., 2000; Kravchinsky et al., 2003). Specific studies identified fine-grained biogenic magnetite as one carrier of the magnetic signal in bottom sediments (Peck and King, 1996), which may, however, be susceptible to reductive diagenesis (Snowball, 1994). Peck et al. (1994) have also shown that magnetic properties are linked to climatic variations with biogenic dilution during interglacial periods and with the increase of terrigenous high-coercivity minerals during glacial periods. For post-depositional processes, Dearing et al. (1998) have shown a weak reductive diagenesis.

The goal of this study is to better understand the links between detrital input, biogenic productivity and early diagenesis, which influence the rock-magnetic signal. This in turn allows us to validate the paleomagnetic variations recorded in Lake Baikal sediments (Demory et al., 2005-this issue), while ensuring a more critical interpretation of the signal carried by rock magnetic parameters. For this purpose, we carefully defined the magnetic mineralogy of different sediment cores of Lake Baikal and compared them to other sediment characteristics such as organic carbon, water, opal, iron and titanium contents.

## 2. Material and methods

Lake Baikal (eastern Siberia) is a rift valley lake located at 51 °N–56 °N and 104 °E–110 °E. It consists of three deep basins separated by two ridges (Fig. 1) with a 7.5-km-thick sediment cover accumulated since the Miocene (Hutchinson et al., 1992). The major catchment area of Lake Baikal is located to the east–southeast. The hinterland is mainly composed of batholiths largely of granitic composition (e.g., Antipin et al., 1997), which provide many kinds of magnetic minerals. The Lake Baikal sediments are built up from detrital input and biogenic productivity, which are modulated by climatic conditions. The biogenic silica production is very low during glacial/stadial periods and high during interglacial/interstadial periods and outlines therefore the climatic variations associated with the expansion and retreat of northern hemisphere ice sheets (BDP-93 and Members, 1994; Colman et al., 1995; Grachev et al., 1997; Prokopenko et al., 2001).

Six sites were cored on geomorphologic highs on the margins of the basins (Fig. 1) to be far from turbiditic and river influences. Hence, the detrital input is mainly influenced by westerly and local winds, which are also likely to be the main source of transport for eolian sediment input into Baikal. Three piston and two pilot cores retrieved from three sites at Academician Ridge during a coring campaign in 1998 and three piston and three pilot cores retrieved during a coring campaign in 2001 were investigated (Table 1). Coring locations of 2001 are the Continent Ridge close to the northern basin (site CON 01-603), the Posolsky Bank between the central and the southern basin (site CON 01-604) and the Vydrino Shoulder on the southern flank of the southern basin (site CON 01-605). Due to the coring method, the uppermost sediments of the piston cores were lost. Where possible, the sedimentary column was completed by a combination of pilot and piston cores (see Demory et al., 2005-this issue).

Rock magnetic samples were continuously taken using 6.2 cm<sup>3</sup> cubic plastic boxes (Table 1). The anisotropy of magnetic susceptibility (AMS) was measured using a Kappabridge KLY-3S (AGICO Brno, Czech Republic). The AMS ellipsoid is characterised by its three principal axes  $k_{\max}$ ,  $k_{\text{int}}$ ,  $k_{\min}$ , and their dip and azimuth. The AMS orientation

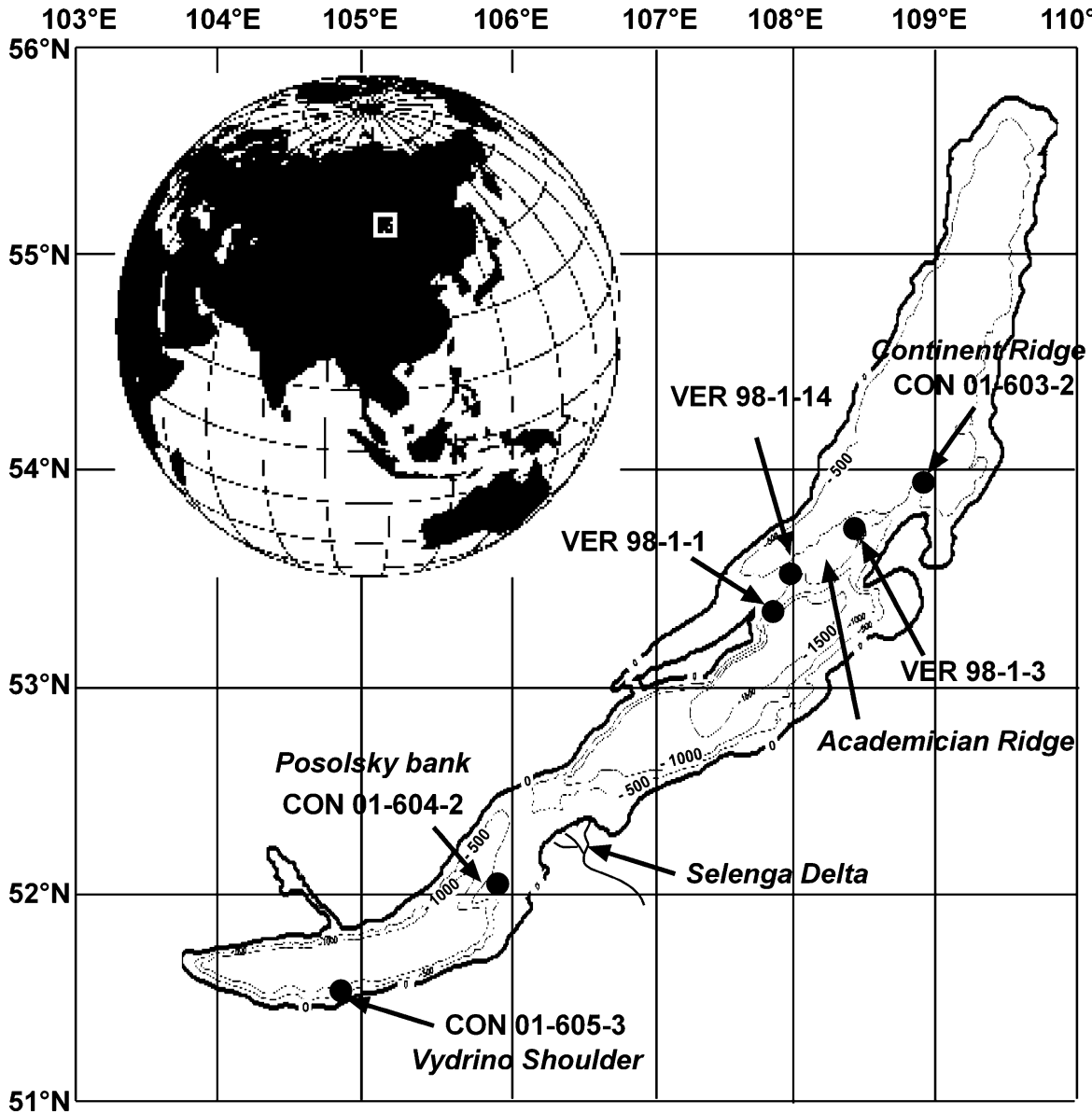


Fig. 1. Simplified bathymetric map of Lake Baikal. The six core locations are marked by black dots.

gives, as a first approximation, the preferred orientation of the magnetic grains and therefore the orientation of the sedimentary fabric (e.g., Rees, 1965; Frank et al., 2002). In unlaminated sediments, the orientation of the AMS axes indicates whether the coring is perpendicular to the sedimentary deposits, thereby allowing the determination as to whether there is any evidence for natural deformations of the

sedimentary fabric. Furthermore, the shape of the AMS ellipsoid is informative, as an oblate shape is typical for compacted sediments, whereas a prolate shape could reflect any deformation of the sedimentary fabric.

Low field magnetic susceptibility ( $\kappa_{LF}$ ) was measured in order to estimate the contribution of ferrimagnetic particles in the sediments.

Table 1

Name, type and length of sediment cores presented in this study as well as their location, water depth and number of discrete rock magnetic samples

Core name and type	Location	Water depth (m)	Latitude	Longitude	Length (cm)	Number of samples
VER 98-1-14 Piston	Academician Ridge	412	53°31'23"N	107°58'10" E	983	383
VER 98-1-14a Pilot	Academician Ridge	412	53°31'23"N	107°58'10" E	192	80
VER 98-1-3 Piston	Academician Ridge	373	53°44'56"N	108°19'02" E	831	331
VER 98-1-1 Piston	Academician Ridge	245	53°23'36"N	107°55'22" E	1120	470
VER 98-1-1a Pilot	Academician Ridge	245	53°23'36"N	107°55'22" E	100	41
CON 01-603-2 Piston	Continent Ridge	386	53°57'48"N	108°54'47" E	1127	479
CON 01-603-2a Pilot	Continent Ridge	386	53°57'48"N	108°54'47" E	190	82
CON 01-604-2 Piston	Posolsky Bank	133	52°04'46"N	105°51'27" E	622	268
CON 01-604-2a Pilot	Posolsky Bank	133	52°04'46"N	105°51'27" E	188	82
CON 01-605-3 Piston	Vydrino Shoulder	675	51°35'06"N	104°51'17" E	1052	453
CON 01-605-3a Pilot	Vydrino Shoulder	675	51°35'06"N	104°51'17" E	173	74
					Total:	2743

Anhyseretic remanent magnetisation (ARM) measurements, free of the effect of the dia-, para- and superparamagnetic components, provide an estimation of the magnetic remanence carriers, mainly of single-domain (SD) grain size.

The isothermal remanent magnetisation (IRM) acquired in a 2-T direct current (DC) field using a pulse magnetiser is defined as the saturation isothermal remanent magnetisation (SIRM). After applying this maximum field, all the samples were magnetised in a field of 300 mT in the opposite direction. The fraction of high-coercivity magnetic minerals was estimated by calculation of the ratio (Bloemendal et al., 1992):

$$S - \text{ratio} = \frac{1}{2} \left( 1 - \frac{\text{IRM}_{-0.3\text{T}}}{\text{SIRM}_{2\text{T}}} \right)$$

S-ratio values range from 0 to 1. The value 1 is obtained for pure magnetite or greigite and decreases with increasing proportion of antiferromagnetic particles such as hematite.

The quantity of high-coercivity minerals (hematite or goethite) was estimated by the high isothermal remanent magnetisation (HIRM), which results from the following relationship:

$$\text{HIRM} = (\text{IRM}_{2\text{T}} - \text{IRM}_{0.3\text{T}})/2$$

This parameter has been used to estimate the detrital input, e.g., eolian input in ice records (Maher

and Dennis, 2001) or in Lake Baikal sediments (Peck et al., 1994) despite discussions about its accuracy (Liu et al., 2002).

Hysteresis loops and backfield curves were determined for a representative population of samples using an Alternating Gradient Force Magnetometer (AGFM, Princeton Measurements model 2900 Micro-Mag). For this purpose, samples were freeze-dried and gently mortared and mixed with an Agar jelly agent suspension and solidified in a 3×3-mm cylindrical mould. The coercive force ( $B_c$ ) and the ratio of saturated remanent magnetisation ( $M_{rs}$ ) and saturation magnetisation ( $M_s$ ) were determined from the hysteresis loop measurements. The coercivity remanence ( $B_{cr}$ ) was deduced from the backfield curves of the saturated samples. The hysteresis parameters indicate the domain status of ferromagnetic particles (e.g., Day et al., 1977), which is linked to the absolute grain size and shape when magnetite dominates the signal (Dunlop, 2002a,b).

High temperature measurements of magnetic susceptibility were performed on 13 representative samples using the same equipment as for  $\kappa_{LF}$  and AMS. Samples showing occurrence for greigite were especially targeted. Indeed, thermomagnetic measurements are generally performed on previously dried sediments, whereas it is known that greigite can be unstable on contact with air (Oldfield et al., 1992). Therefore, relevant thermomagnetic curves were obtained only on wet sediments from the intervals where greigite was suspected. Thermomagnetic

curves for these wet samples were determined using a “Variable Field Translation Balance” (VFTB), which is a combination of a Curie balance with a vibrating sample magnetometer (Nowaczyk et al., 2000). The measurement was performed at saturation magnetisation and in an argon atmosphere.

Magnetic extracts were analysed by X-ray diffraction and transmission electronic microscopy (TEM) using a STOE Stadi P diffractometer and a Philips CM200 transmission electron microscope, respectively. Magnetic minerals were extracted from an interval dominated by magnetite at depth 527.5–529.9 cm (clay-rich layer) and one from an interval dominated by hematite at depth 583–590 cm (diatomaceous layer) in core VER 98-1-1. The extraction was done after removal of the organic carbon, using a magnetic needle plunged in the sediment suspended in water in an ultrasonic bath. The goal was to better constrain the rock magnetic results where the X-ray analysis gives a semiquantitative characterisation of the components of the magnetic extract (Rietveld structure refinement method using the program GSAS, see Larson and Von Dreele, 1987) and the TEM allows magnetic grain size to be directly observed and to proceed to elemental dispersive spectra on specific minerals.

We measured on the same cores water, opal, total organic carbon (TOC), total sulphur (TS), (relative) iron and (relative) titanium contents. The water content was determined from samples retrieved with cylindrical syringe samplers, weighed wet and weighed again after freeze-drying. Opal content was obtained by measuring the  $\text{NaCO}_3$  leached solution by inductive coupled plasma with an optical emission spectrometer (ICP-OES). Total organic carbon (TOC) and total sulphur (TS) were determined using a LECO CS-225-Analyser. A semiquantitative estimate of titanium, iron and sulphur contents was obtained on selected intervals, using X-ray fluorescence (XRF) logging at 2-mm steps (Jansen et al., 1998).

### 3. Sedimentary fabric

Visual screening of sediments to determine disturbances was successful whenever laminations occurred. As sediments of Lake Baikal are often unlaminated, we estimated the bedding direction by

measuring the orientation of magnetic minerals using AMS. The AMS data are plotted in a stereographic projection (Fig. 2). As most AMS data plot with long axes at  $0^\circ$  and short axes at  $90^\circ$ , an overall horizontal stratification is evident. However, for a few samples, the short axis of AMS deviates from the vertical orientation, indicating oblique laminations which are either due to coring artefacts, as observed at the very top or bottom of the cores, or due to earthquake-induced slumps (Oberhänsli, 2000), with earthquakes being common in the Baikal rift valley (Sherman and Gladkov, 1999).

Furthermore, a slight preferential orientation parallel to the  $0^\circ$  direction of the stereographic projection is observed for the long axis of magnetic anisotropy (Fig. 2). As the samples were not geographically oriented, we interpret this preferred orientation to be a sampling artefact resulting from a slight shearing when the plastic box penetrates the sediment during subsampling rather than indicating paleocurrent directions (Oda et al., 2002).

In conclusion, the AMS results document that the sediments under investigations are mostly undisturbed, and given the oblate shape of the AMS ellipsoids (Fig. 2), compaction has been effective.

### 4. Lithological variations and ARM

The typical Baikal sedimentary succession consists of clay-rich layers alternating with diatomaceous layers, indicating glacial (cold) and interglacial (warm) periods, respectively (BDP-93 and Members, 1994; Colman et al., 1995; Grachev et al., 1997; Fig. 3). The clay-rich layers are characterised by a high ARM and low levels of TOC, TS, opal and water. The diatomaceous layers, indicating high-biogenic productivity, show low ARM and high levels of TOC, TS, opal and pore water. Instead of using the magnetic susceptibility ( $\kappa_{LF}$ ) for monitoring the varying concentration in magnetic minerals (e.g., Sakai et al., 2000), we used ARM to counter smoothing of the magnetic susceptibility signal by high contents in diamagnetic opal. Correlating the ARM from Lake Baikal cores with the orbitally tuned  $\delta^{18}\text{O}$  curve from ODP 677 (Shackleton et al., 1990), we identified marine isotope stages (MIS; Fig. 3) and estimated the time span recorded in sediments.

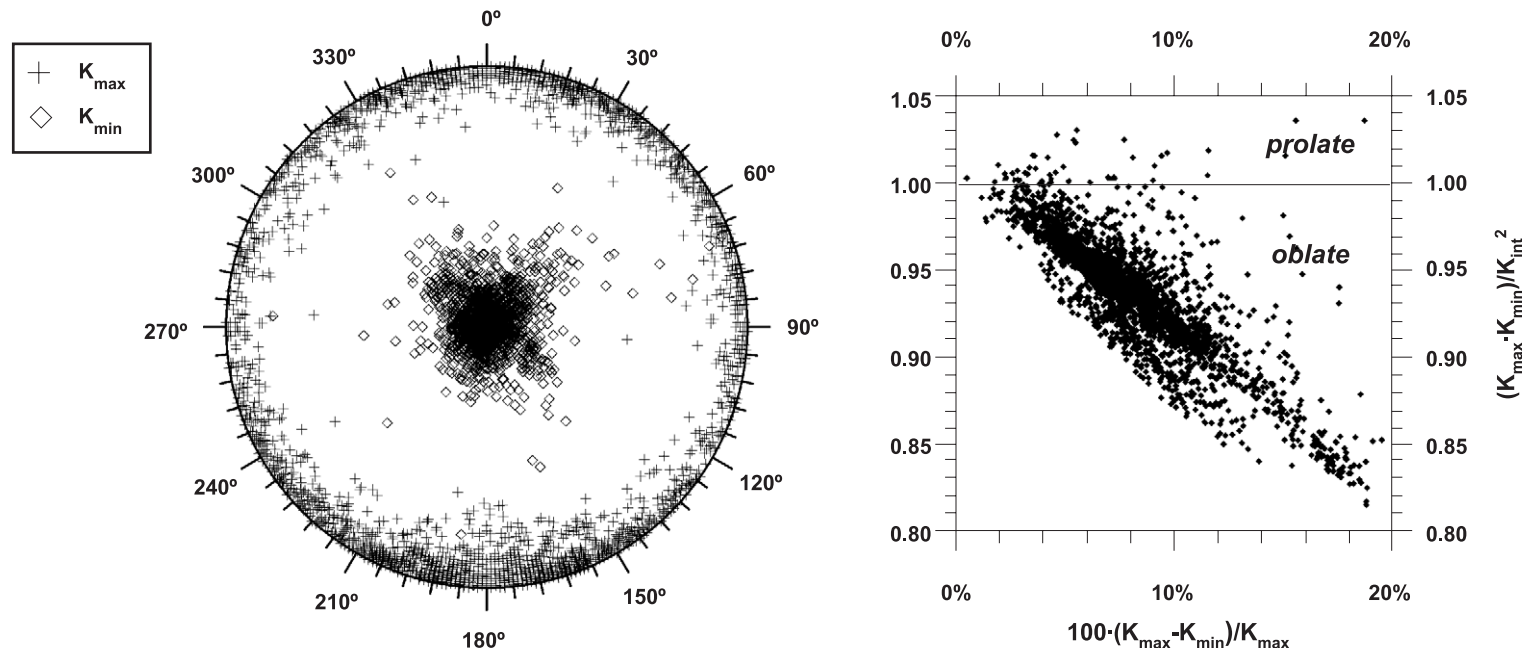


Fig. 2. Stereographic projection of the minimum ( $k_{\min}$ ) and maximum ( $k_{\max}$ ) axes of the AMS ellipsoid and diagram of the shape of the AMS ellipsoid (Stacey et al., 1960) vs. the degree of magnetic anisotropy (Graham, 1966) for all cores.



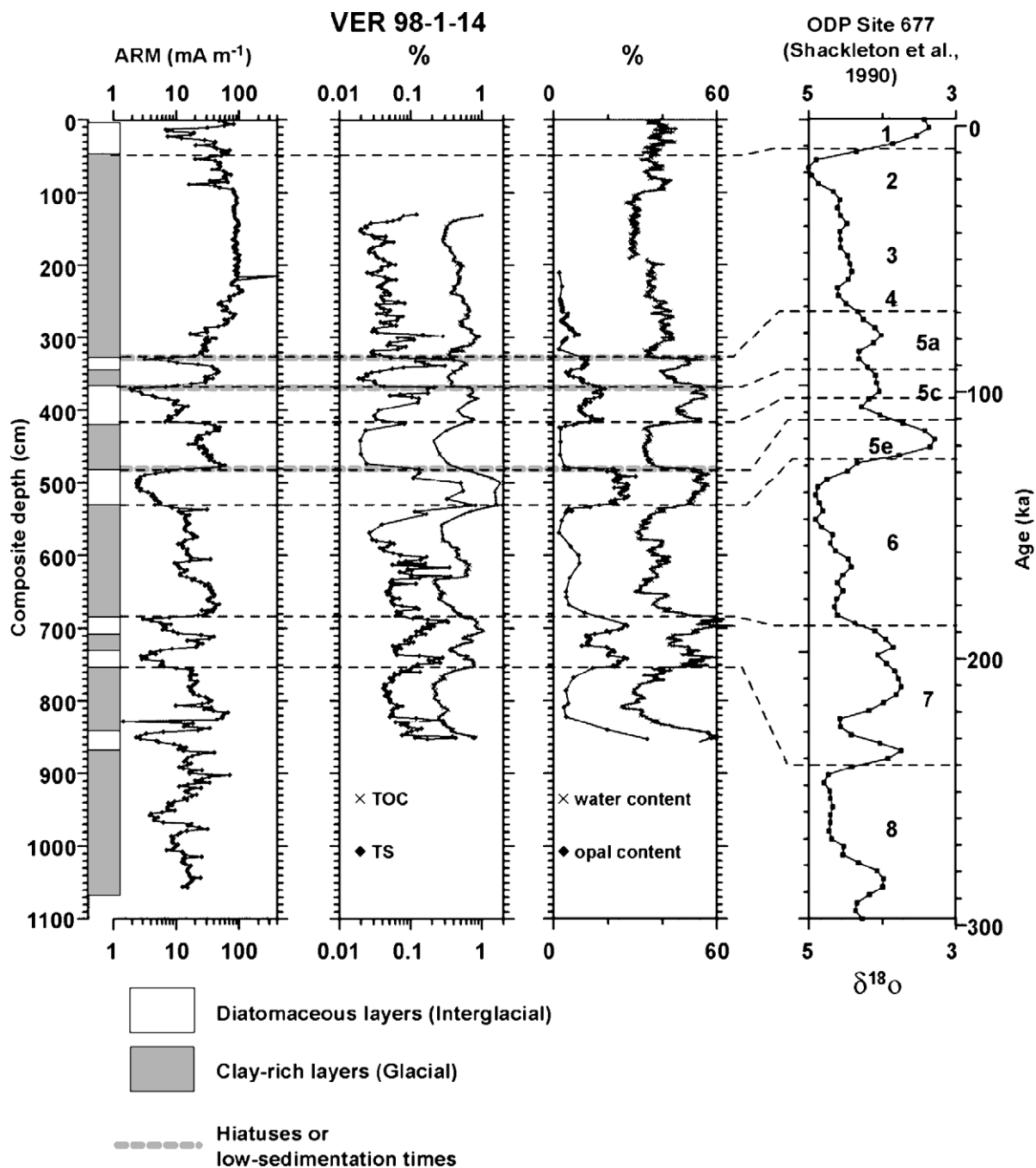


Fig. 3. Downcore variations of the ARM, TOC, water and opal content and simplified lithology for the sedimentary sequence of VER 98-1-14. Correlation to MIS using the  $\delta^{18}\text{O}$  variations measured in ODP Site 677 by Shackleton et al. (1990).

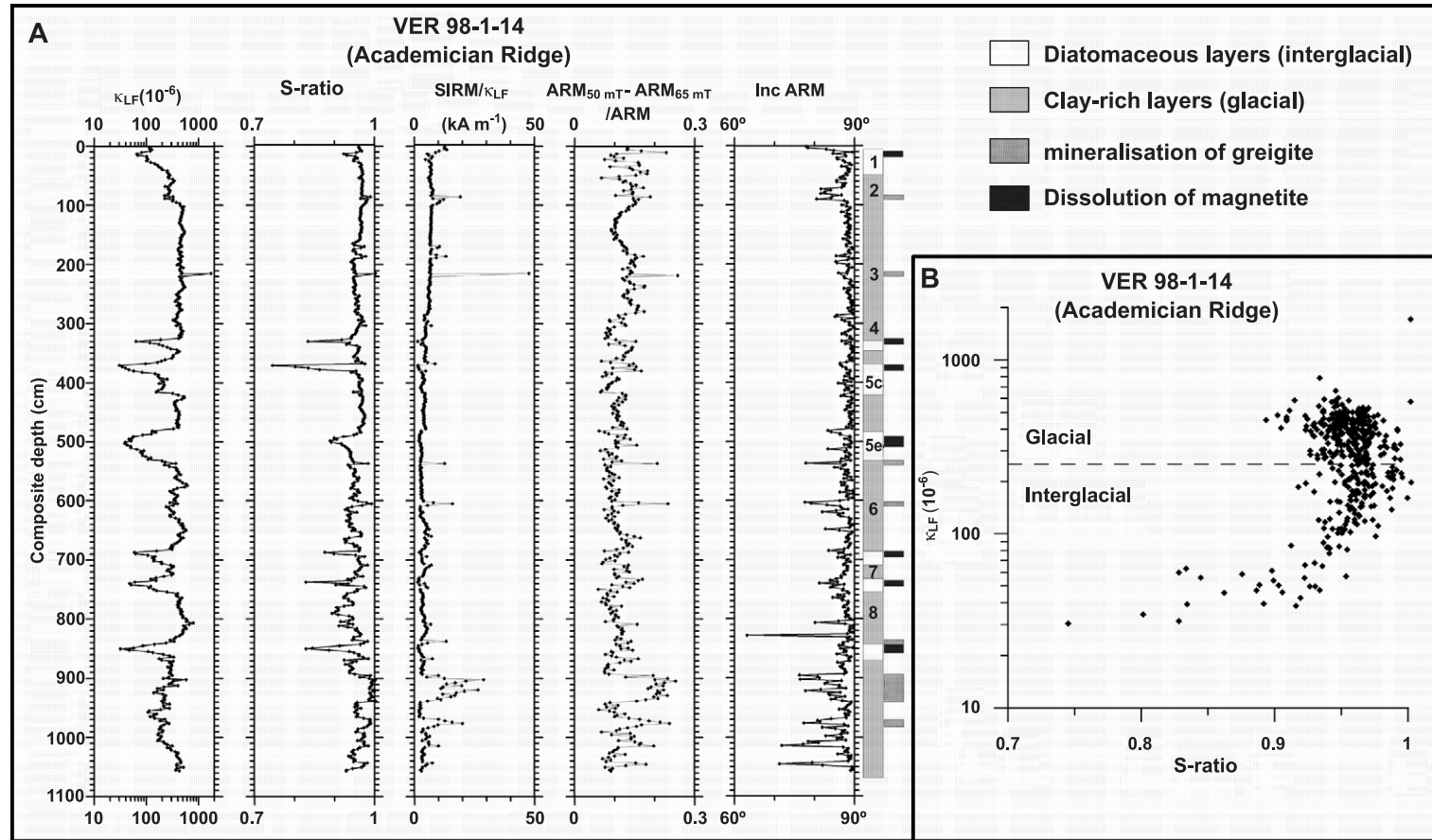


Fig. 4. (A) Downcore variations of rock magnetic parameters and simplified lithological description for the sedimentary sequence VER 98-1-14. Here, MIS are denoted by numbers in the lithological column. The black squares filled intervals mark occurrences of greigite characterised by a high magnetic susceptibility ( $\kappa_{LF}$ ) in parts, with a low coercive mineral dominating the magnetic signal (S-ratio close to 1), a high SIRM/ $\kappa_{LF}$ , a strong loss of ARM intensity between the demagnetisations steps 50 and 65 mT and finally a deviation of the inclination of ARM. The dark grey intervals mark occurrences of magnetite dissolution, with a low S-ratio resulting from relative higher hematite content in the ferromagnetic components. The assignment of greigite and dissolved magnetite is based on subsequent interpretation. (B) Magnetic susceptibility ( $\kappa_{LF}$ ) vs. S-ratio for the sedimentary sequence VER 98-1-14 showing S-ratio gathered around 0.95 in glacial sediments and scattered from 0.7 to 1 in interglacial sediments.



The ARM records also allow cores from different sites across Lake Baikal to be correlated (Fig. 3). Sediment discontinuities as suggested by lithological descriptions at several transitions from interstadial to stadials are marked by abrupt changes in ARM. We show later in this paper that these periods of low or no sedimentation strongly influence the magnetic mineralogy.

## 5. Magnetic mineralogy—results

Fig. 4A shows variations of different rock magnetic parameters in one core in order to assess the magnetic mineralogy, as described hereafter. The magnetic susceptibility does generally not exceed  $500 \times 10^{-6}$  SI, except at certain depths where peak values are about one order of magnitude higher. The S-ratio is rather constant with values around 0.95 over the whole depth range. Still, some lower values of about 0.75–0.85 are observed, coinciding with low susceptibility values. At certain depths, the S-ratio is close to 1, e.g., between 900 and 940 cm.  $SIRM/\kappa_{LF}$  is constantly low, apart from single peaks which correlate with the highest S-ratios. The parameter indicating an ARM loss between 50 and 65 mT has a similar pattern than  $SIRM/\kappa_{LF}$ , but it is much more influenced by noise. The inclination of the acquired ARM is  $\sim 90^\circ$ , apart from some exceptions. Lower inclination occurs sporadically and correlates partly (e.g., at 890–940 cm) with S-ratio,  $SIRM/\kappa_{LF}$  and  $ARM_{50mT}-ARM_{65mT}/ARM$  maxima. Fig. 4B shows that magnetic susceptibility is high in glacial and low in interglacial intervals. In addition, it shows that the S-ratio varies less in glacial sediments, ranging from 0.9 to 1, than in interglacial sediments where the S-ratio is scattered from 0.7 to 1.

In order to understand the previously described stratigraphic variations, we performed thermomagnetic analyses (susceptibility and induced magnetisation) from characteristic depths. Fig. 5A shows the temperature dependence of magnetic low-field susceptibility for a sample from a clay-rich layer with an S-ratio of  $\sim 0.95$ ,  $\kappa_{LF}$  of  $\sim 500 \times 10^6$  SI, low value  $SIRM/\kappa_{LF}$  and no deviation of the ARM inclination. The susceptibility remains constant until 400 °C, then increases until a peak value at  $\sim 560$  °C and decreases

rapidly until 610 °C. The sample in Fig. 5B originates from a diatomaceous layer (low susceptibility and S-ratio). The susceptibility decreases steadily until 670 °C when the signal is lost. The samples in Fig. 5C and D come from depths where almost all magnetic parameters have peak values (see Figs. 4 and 12). Both graphs indicate a clear maximum at 300 °C. The magnetisation then decreases until 600 °C; above this temperature, the magnetisation is zero. It should be noted that all curves are irreversible, indicating the thermal instability of the magnetic minerals present.

Fig. 6A shows hysteresis measurements of three samples with different S-ratios. The highest saturation magnetisation ( $M_s$ ) and coercive force ( $B_c$ ) was observed in the sample with an S-ratio  $>0.95$ , the lowest  $M_s$  and  $B_c$  in the sample with an S-ratio  $<0.9$ . In all cases, the hysteresis curve is influenced by paramagnetism, the effect being largest in the sample with low S-ratio. The day plot (Fig. 6B) indicates that samples with S-ratios  $>0.95$  plot rather in the single-domain (SD) to pseudosingle-domain (PSD) range. Samples with S-ratios between 0.9 and 0.95 instead, plot rather in the PSD to the multidomain (MD) range. Low S-ratio samples are not greatly dispersed and have ratios of  $B_{cr}/B_c$  and  $M_{rs}/M_s$  of 3.5 and 0.1, respectively.

## 6. Magnetic mineralogy—interpretation

Three different magnetic mineral populations seem to be present in the sediment cores from Lake Baikal. The temperature dependence of magnetic susceptibility indicates a magnetite/maghemite population for S-ratios between 0.9 and 0.95, which is probably of detrital origin because it occurs in clay-rich sediments deposited during glacial-periods (Fig. 3). Energy dispersive X-ray spectroscopy (EDS) on transmission electronic microscopy (TEM) indicates an enhanced iron and oxygen content in analysed grains (Fig. 7), which are suggested to consist of iron oxides. The X-ray diffraction (XRD) spectra from magnetic extracts of clay-rich layers (Fig. 8A) support the previous suggestion, indicating magnetite as dominant mineral. S-ratios close to 1 indicate the absence of a high-coercivity mineral component. The Curie temperature measurements (Fig. 5C and D) show a loss of remanence above 300 °C, which is typical for the

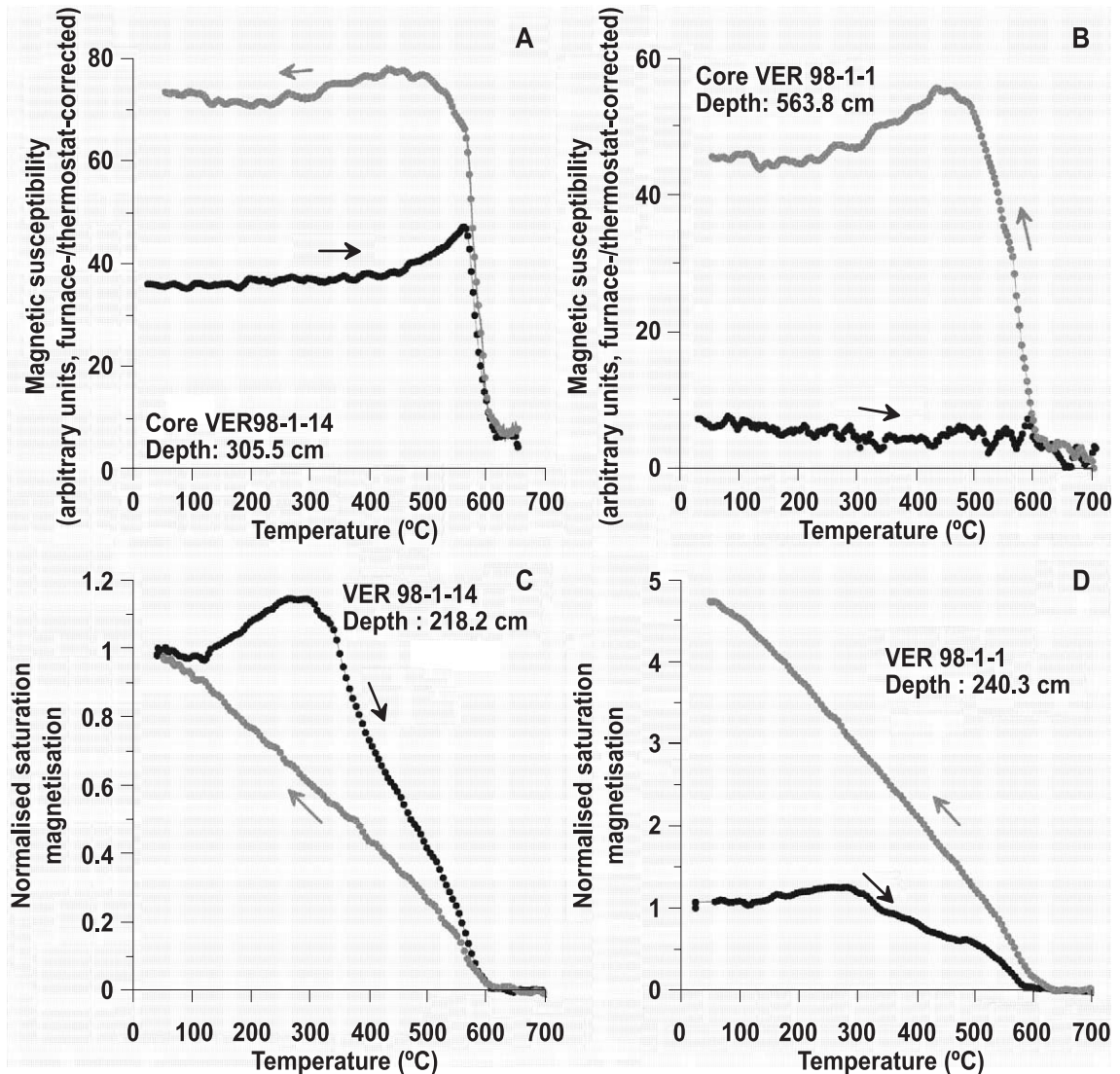


Fig. 5. (A) High temperature measurements of magnetic susceptibility in clay-rich layers: magnetite characterised by a Curie temperature of 590 °C dominates the signal. (B) High temperature measurements of magnetic susceptibility in diatomaceous layers: most of the weak susceptibility is still present up to the temperature of 670 °C and carried by hematite. (C and D) High temperature measurements of the saturation magnetisation, both samples show a loss of a part of the signal at temperatures between 350 and 400 °C, typical disintegration temperatures for greigite. The remaining signal disappears above a temperature of 590 °C, typical for magnetite.

mineral greigite (Roberts, 1995). The hysteresis loop indicates a coercive force of ~45 mT, which is in agreement with greigite data from Roberts (1995), in line with other hysteresis parameters. Deflections from the ARM axis can be caused by a gyroremanent magnetisation acquired during static AF demagnetisation in anisotropic samples (Stephenson, 1980).

Such gyroremanence has been identified in natural greigite samples (Hu et al., 1998, 2002; Stephenson and Snowball, 2001). According to Roberts (1995) and Oldfield (1998), both a high SIRM/ $\kappa_{LF}$  and the absence of a hard remanence component in combination with strong gyroremanences are typical for authigenic greigite.

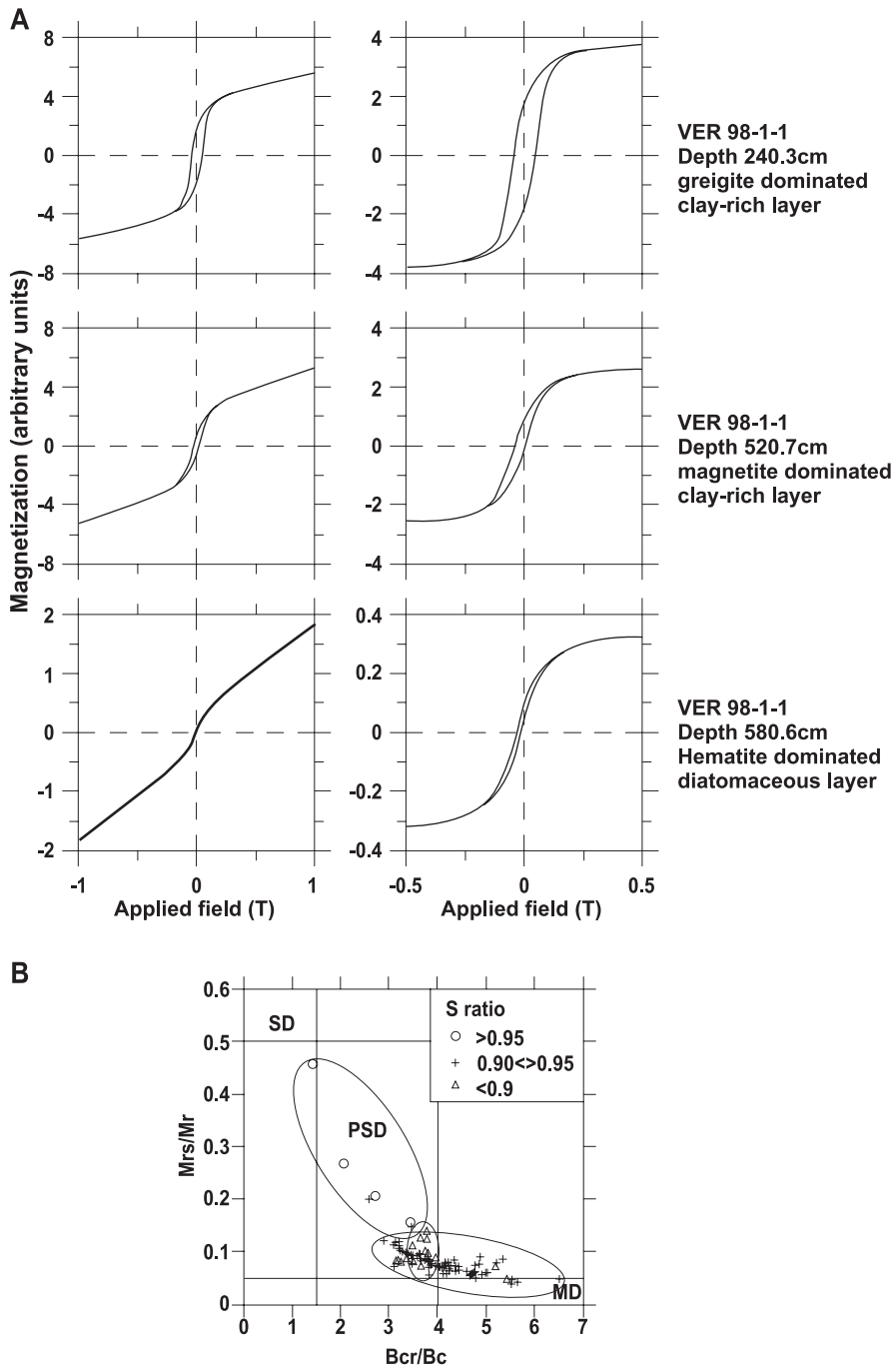


Fig. 6. (A) Three characteristic hysteresis loops uncorrected (to the left) and corrected for the paramagnetic influence (to the right). On top a single-domain behaviour hysteresis loop for a sample with occurrence of greigite, in the middle a pseudosingle-domain behaviour of the hysteresis loop from a clay-rich layer and below a pseudosingle to multidomain behaviour of the hysteresis loop from a diatomaceous layer. (B) Day plot (Day et al., 1977) of hysteresis parameters of representative samples with the boundaries between single-domain (SD), pseudosingle-domain (PSD) and multidomain (MD) area. We classified the samples according to their S-ratio (see the three ellipses).

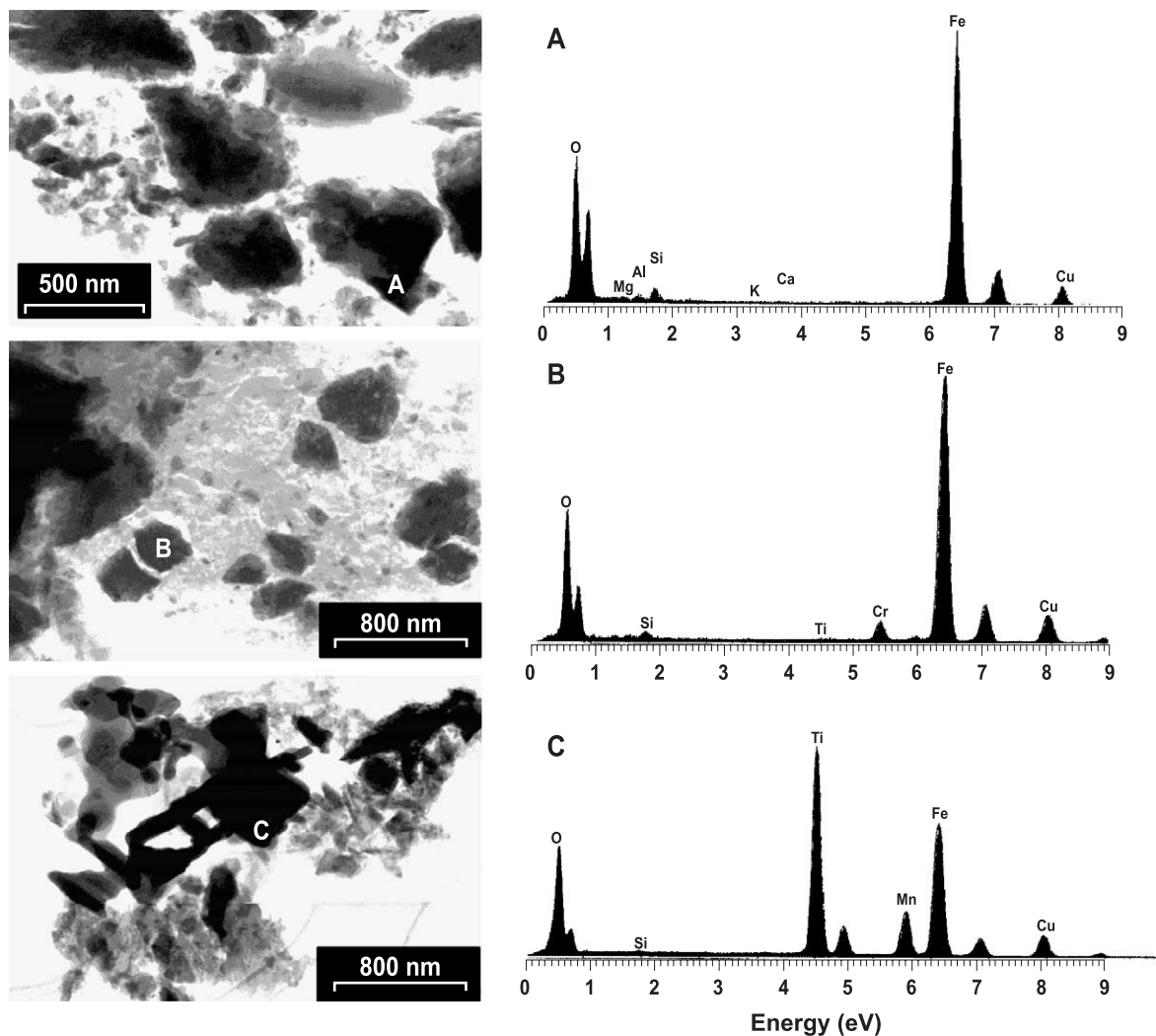


Fig. 7. Representative transmission electron microphotographs and elemental dispersive spectra of magnetic extract. Oxides of different size (from submicron to micron) are visible on the microphotographs. (A) In the clay-rich layer, the extract is dominated by pure iron oxides (magnetite). (B and C) In the diatomaceous layer (interval 583–590 cm, core VER 98-1-1), there is a relative enrichment in titanium and chromium of the oxides.

The interpretation of samples with low S-ratios is rather difficult. Low S-ratios indicate the presence of a high-coercivity component, i.e., grains with remanent coercive forces  $>300$  mT. We tend to interpret it as a signal of hematite based on thermomagnetic curves (Fig. 5B), while the hysteresis loop contradicts the S-ratio. The measured coercive force ( $B_c$ ) in Fig. 6A (lowermost loop) is about 11 mT only. According to the ratio  $B_{cr}/B_c$ , the remanent coercive force would be

around 40 mT. Hematite with such small  $B_c$  is of multidomain size and about 1  $\mu\text{m}$  in diameter (Kletetschka and Wasilewski, 2002) and should be remagnetised when applying an opposite field during the S-ratio procedure. Nevertheless, the S-ratio is low, and we suggest that the presence of a certain amount of superparamagnetic magnetite/maghemite particles is lowering the coercive force. These superparamagnetic grains would not affect the S-ratio as they are not

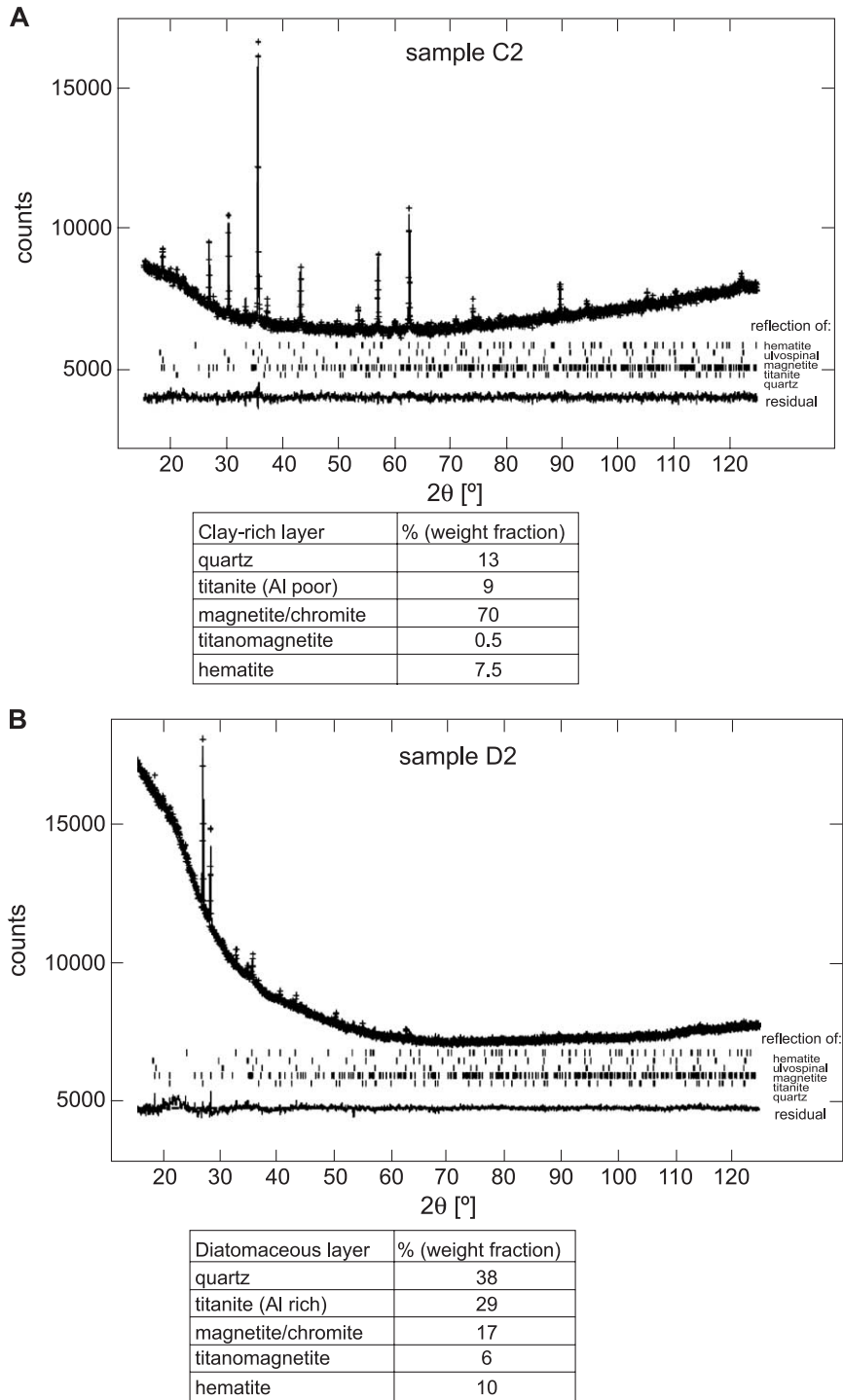


Fig. 8. X-ray diffraction patterns and semi-quantitative approach of the different phases for magnetic extracts. (A) Extract from the clay-rich layer, characterised by 70% of magnetite and by a titanite poor in aluminium. (B) Extract from diatomaceous layer, characterised by only 17% of magnetite and by a titanite rich in aluminium.



able to carry a remanent magnetisation. Indeed, the TEM microphotographs in Fig. 7B show that grains in the superparamagnetic grain size range are present in the diatomaceous layers. They are probably relics of biogenic magnetite, which has formed at the water/sediment interface, as has been described by Peck and King (1996). In addition, there are also grains containing titanium (Fig. 7C), indicating substitution of titanium for iron oxide. This is confirmed by XRD analysis (Fig. 8B), which shows a relative abundance of titanite and titanomagnetite while the magnetite content is much less.

## 7. Discussion

The magnetic mineralogy demonstrates that magnetite, probably of detrital origin, dominates the signal in most of the glacial sediments, except in a few intervals characterised by the presence of greigite. The interglacial sediments present different magnetic mineral assemblages with predominance of either magnetite (sometimes with greigite) or hematite.

In this section, we compare the magnetic mineralogy with nonmagnetic proxies such as water, opal, TOC and TS wt.%, semiquantitative Fe and Ti contents. These proxies trace the biogenic productivity and the detrital input but are also indicative of early diagenetic conditions, which control, e.g., the preservation of organic matter and the redox conditions, and would help to constrain the processes responsible for modifications in magnetic mineral assemblages.

### 7.1. Tracers of the detrital input

In selected intervals, we measured titanium and iron contents in parallel to rock magnetic parameters (Fig. 9). Titanium content is a good reflection of detrital input since minerals containing titanium are not very sensitive to dissolution. Iron, however, is rather mobile and involved in the redox history of highly porous sediments: the spike of iron observed on top of the sedimentary column (Fig. 9A) marks the redox front. We observed a strong similarity between the titanium and HIRM curves: the detrital input decreases from the late glacial to the Hol-

ocene. In ancient sediments, HIRM and titanium display similar variations with high values in glacials and low values in interglacials (Fig. 9B). Notably, no significant HIRM change is observed at the transition between oxidising and reducing conditions in the sediment (Fig. 9A). This implies that HIRM is not affected by redox conditions and further confirms that the “hard” magnetic mineral content is the best tracer of detrital input (Peck et al., 1994). On the other hand, the S-ratio seems to be related to the redox conditions in the sediment (see Section 7.2). The ARM has also to be considered with caution as it is mainly influenced by the ferrimagnetic contribution, which is itself influenced by post depositional processes. This is seen in Fig. 9 where ARM variations are partly influenced by S-ratio variations.

### 7.2. Dissolution of magnetic minerals

The difference by an order of magnitude between ARM values in glacial and interglacial sediments (Fig. 3) suggests the dissolution of magnetic minerals in the sediment. The observed difference cannot result only from low detrital input and dilution of the lithogenic component by opal (30 wt.%) and pore water (40 wt.%; Fig. 3).

The topmost sediments are oxidised since the entire water column of Lake Baikal is oxygen saturated throughout the year (Weiss et al., 1991). High ARMs as well as high S-ratios in this oxidised zone (Fig. 9A) are partly due to fine-grained biogenic magnetite (Peck and King, 1996). The redox boundary between the oxic zone at the top and the anoxic zone below is marked by a downward decrease of the ARM and S-ratio values, while the HIRM (i.e., the quantity of “hard” magnetic minerals such as hematite) remains constant. The decrease in the S-ratio is therefore due to a decrease of “soft” magnetic minerals (magnetite), which is linked to processes in the redox front and results from an in situ process.

Processes driving selective dissolution of “soft” magnetic particles under suboxic and anoxic conditions in the pore water are still debated. In lakes characterised by sediments rich in organic carbon, hematite has been shown to dissolve first (Williamson et al., 1998). In subarctic lakes (Snowball, 1993) and

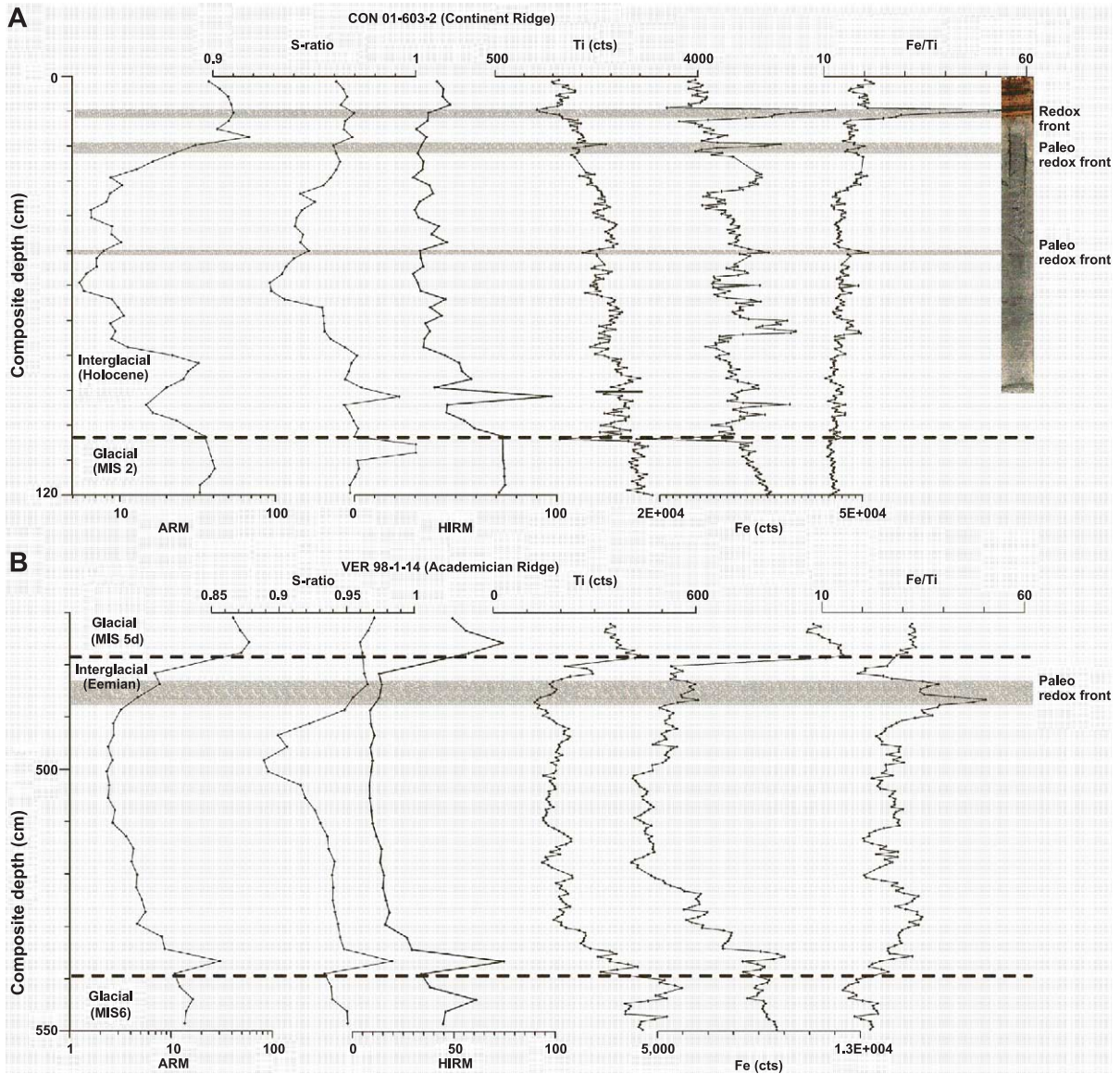


Fig. 9. Downcore variations of rock magnetic parameters (ARM, S-ratio and HIRM), and XRF titanium, iron counting and ratio Fe/Ti for two different sedimentary sequences, redox and paleo-redox fronts, are highlighted in grey. (A) Section at site CON 01-603-2 covering the Holocene and MIS 2; on the photo of the core, the limit oxic/anoxic sediments is well documented. (B) Section at site VER 98-1-14 covering MIS 5d, Eemian and MIS 6.

in Lake Baikal (the present study), the fine grained magnetite dissolves easier than hematite under similar conditions with relatively low organic carbon contents (up to 2 wt.%) and low sedimentation rates. Due to high surface/volume ratio, the small grains of bi-magnetite (Peck and King, 1996) and magnetite, which underwent maghemitization under oxic/suboxic

conditions, are very sensitive to dissolution processes (Smirnov and Tarduno, 2000). The dissolution of soft magnetic minerals (magnetite) after burial below the redox front is probably mediated by bacteria in the presence of organic carbon. We suggest two types of transformation in interglacial sediments of Lake Baikal. First, the dissolution of magnetic minerals is

the main supplier of soluble  $\text{Fe}^{2+}$  feeding the redox front (Granina et al., 2004). Secondly, a high concentration of dissolved opal in the pore water facilitates the transformation of magnetite into smectite (Florindo et al., 2003). This would corroborate the occurrence of a secondary smectite in Lake Baikal sediments (Fagel et al., 2003).

The dissolution of soft magnetic minerals is not only observed in recent sediments but also in other interglacial sediments such as the Kazantsevo (equivalent to the Eemian in Europe; Fig. 9B). We observed low S-ratio below a peak of iron over titanium interpreted as a paleo-redox front. Therefore, dissolution of soft magnetic minerals is a feature also observed in ancient interglacial sediments and may result from similar processes.

Nevertheless, this dissolution is only observed at the end of some interglacial intervals. Dissolution events do not trace a basin-wide signal in Lake Baikal but result from local phenomena since they cannot be correlated from one core to another core. Furthermore, they are observed just below preserved paleo-redox fronts, as highlighted by spikes of iron over titanium (Fig. 9). The paleo-redox fronts are themselves observed just below zones of condensed sedimentation rates. Indeed, several studies have demonstrated a strong relationship between a decrease of the sedimentation rates and preservation of paleo-redox fronts (Deike et al., 1997; Granina et al., 2000, 2004). In the present study, there are further pieces of evidence for changes in the sedimentation rates. According to AMS  $^{14}\text{C}$  measurements (Piotrowska et al., 2004) performed on a Kasten core taken at site CON 01-603-2 and transferred to the present study by susceptibility correlation (Demory et al., 2005-this issue), a general decrease of the sedimentation rates was observed in the topmost section of the sedimentary column:  $\sim 10 \text{ cm ky}^{-1}$  between 98 and 80 cm depth and  $\sim 4.5 \text{ cm ky}^{-1}$  between 25 and 2 cm depth. This decrease is likely to be underestimated since we have not considered the sediment compaction processes. Moreover, abrupt changes between interglacial and glacial sediments may be hiatuses, as in core VER 98-1-14, where we found many events of soft magnetic mineral dissolution and sediment discontinuities (Fig. 3).

Changes in sedimentation rates are also observed in core VER 98-1-1 located on the slope between

Academician Ridge and the central basin (Fig. 1). Interglacial intervals here are very thick and most probably related to redeposition events (Ceramicola et al., 2002), while glacial intervals have similar extension as determined from other cores at the Academician Ridge (Fig. 4). In this core also, the S-ratio decreases strongly on top of interglacial stages (Fig. 10).

Processes responsible for low sedimentation or hiatuses were suggested after high-resolution seismic investigations. Ceramicola et al. (2002) observed many events of winnowing, which could be responsible for sedimentation rate decay, while local slumping cannot be neglected as a cause for hiatuses. The low cohesivity of the highly porous interglacial sediments would easily lead to a destabilisation of the sediments. A decay of the biogenic productivity (less opal input), which would not be immediately compensated by the glacial type detrital input, could be another reason for the sedimentation decrease at the end of interglacials.

### 7.3. Occurrence of greigite

Authigenesis of greigite is another characteristic of the sedimentary sequences of Lake Baikal. As summarized by Dekkers et al. (2000), the greigite can form diagenetically after deposition of sediments during bacterial reduction or when hydrothermal fluids are present. Greigite is more likely to grow beyond the redox front during sulphate reduction, although the influence of hydrothermal fluids activated in the tectonic setting of Lake Baikal cannot be ruled out. Increased presence of greigite (high SIRM/ $\kappa_{\text{LF}}$ ) coincides with maximum sulphur contents observed at the beginning of interglacial stages (Fig. 11A). At similar levels in another sediment core of Lake Baikal, Watanabe et al. (2004) observed pyrite mineralization. They attributed these pyrite-rich levels to mineralization at sediment/water interface under anoxic bottom water conditions. However, we prefer to interpret the greigite as a result of magnetite transformation when sulphate reduction occurs in the interglacial sediments. Peak sulphur contents would therefore be due to sulphur mineralization within the sediment and would not result from an enrichment of the sediment in sulphur at the sediment/water interface.

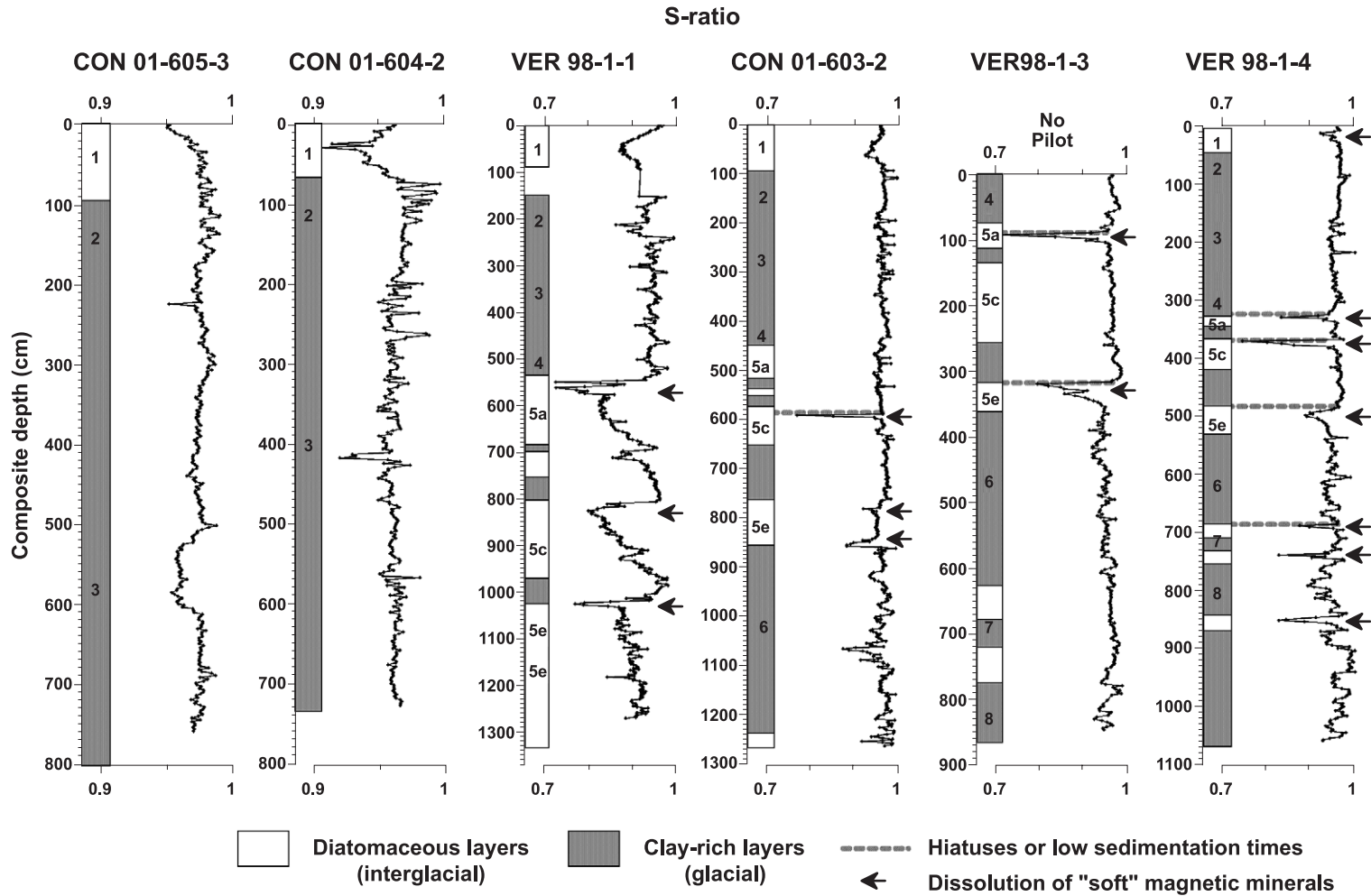


Fig. 10. Downcore variations of the S-ratio and simplified lithological description. Here, MIS are denoted by numbers in the lithological columns. The arrows show spikes of low S-ratios.



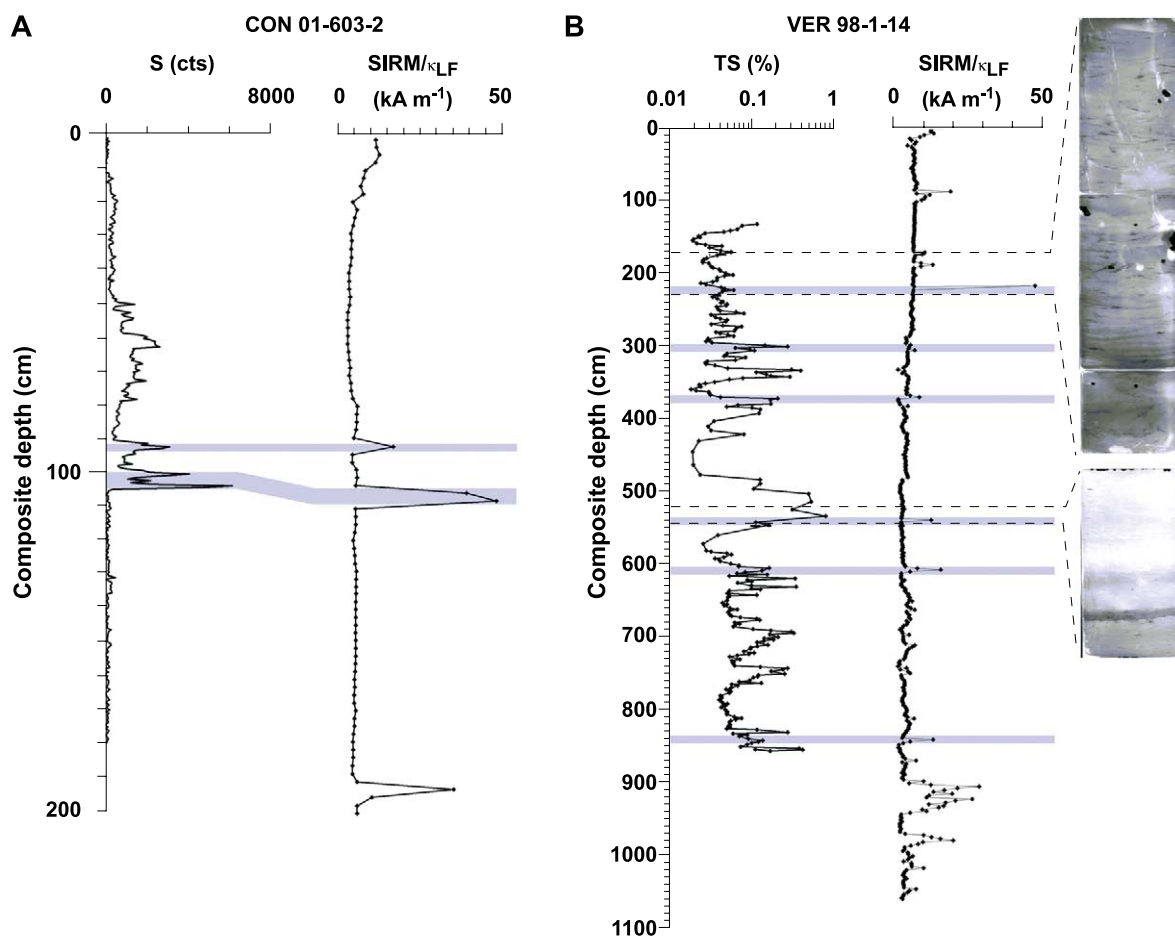


Fig. 11. Downcore variations of sulphur and  $SIRM/\kappa_{LF}$  (high values are considered to indicate greigite). (A) Topmost part of the sedimentary sequence from site CON 01-603-2, relative sulphur content is estimated by XRF counting. (B) Full record for sedimentary sequence from site VER98-1-14, total sulphur content. For panels (A) and (B), the grey lines show the correlation between increase of sulphur and presence of greigite. Two intervals are documented by radiographs showing the scattered distribution of the greigite in glacial sediments and the layer rich in sulphur at the transition glacial/interglacial.

Higher abundance of greigite during glacial intervals also coincides with small increases of the S content (Fig. 11B). Greigite levels in glacial sediments cannot be correlated between cores (Fig. 12), which suggests that greigite concentrations are driven by local processes. We suggest that faecal pellets could be a suitable microenvironment for sulphate reduction. And while greigite could potentially act as proxy for faecal pellets in glacial sediments, unfortunately, we cannot rely on this possible indicator since the greigite is very sensitive to onshore alterations after sampling (Snowball and Thompson, 1990).

## 8. Conclusion

Continuous rock magnetic measurements, complemented by X-ray diffraction and TEM on magnetic extracts, were performed on cores from Lake Baikal covering several glacial and interglacial stages. Compared to geochemical data, the rock magnetic study showed that:

(1) HIRM, i.e., hematite+goethite content, remains the best estimate for the detrital input in Lake Baikal, whereas parameters estimating the magnetic mineral concentration, like magnetic susceptibility or ARM,



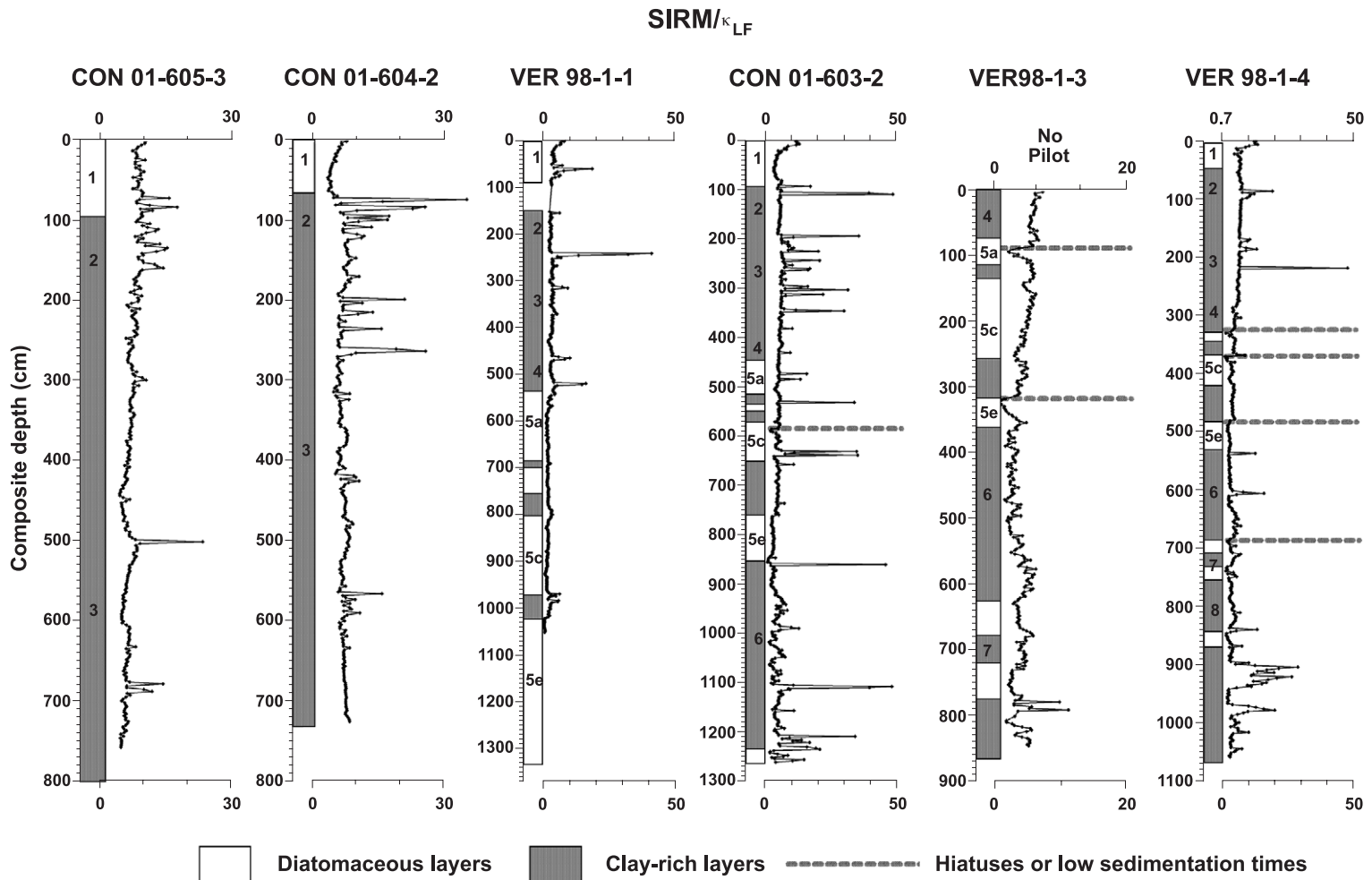


Fig. 12. Downcore variations of the SIRM/ $\kappa_{LF}$  (high values are considered to indicate greigite) and simplified lithological description. Here, MIS are denoted by numbers in the lithological columns.

are partly influenced by postdepositional processes such as magnetic dissolution.

(2) Magnetite dominates the magnetic signal in glacial sediments except for a few enhancements of greigite, probably confined to reductive microenvironments.

(3) Magnetic assemblages vary in interglacial sediments with predominance of magnetite+greigite at the beginning of interglacial intervals and a predominance of hematite at the end of some of the interglacial intervals. For interglacial sediments, we propose a model of the magnetic signal involving mainly in situ processes. Due to less wind, the detrital input in Lake Baikal is low compared to the glacial, and therefore, there are less detrital magnetic minerals as observed in the HIRM curves (Fig. 9). During interglacial stages, the biogenic productivity is high, and the bottom water of Lake Baikal is known to be well oxygenated. In the oxidised bottom sediments, a magnetite is generated by magnetotactic bacteria (Peck and King, 1996). After burial, the biomagnetite is passed by the redox front (rich in iron) and then stays in a suboxic to anoxic environment where organic carbon is preserved. In the case of constant sedimentation rates, the burial is quite fast. Consequently, the magnetite could be preserved or transformed into greigite once sulphate reduction occurs. This scenario is proposed for the beginning of the interglacials. A second scenario occurs when the sedimentation rate decreases. In this case, magnetite stays longer just below the redox front. This allows a slow dissolution of magnetite and a significant precipitation of iron at the redox front. This is expressed by the preservation of a paleo-redox front, as observed in the present study as well as in previous studies (e.g., Deike et al., 1997; Granina et al., 2004) and by low S-ratios, showing the preferential dissolution of soft magnetic minerals. Low S-ratios can therefore be used as a toll for tracing decreases of the sedimentation rates which occur at the end of some of the interglacial period.

## Acknowledgments

This work was done in the frame of the project CONTINENT supported by the European Commission under contract EVK2-CT-2000-00057.

We thank Frederich Heller, David Williamson and Simo Spassov for their fruitful comments on the manuscript. Holger Lippitz helped with AMS measurements and Sushma Prasad, Anon Mackay and Jens Klump for correcting the English.

## References

- Antipin, V.S., Tomilov, B.V., Goreglyad, A.V., Kovalenko, V.I., Budnikov, S.V., 1997. Chemical composition of granitoids of the Angara–Vitim batholith as a source of sediments in the eastern part of Lake Baikal. *IPPCCE Newsl.* 10, 5–16.
- BDP-93 and Members, B.D.P., 1994. First data of the first drilling on Lake Baikal, Buguldeika Site, Southeastern Siberia. *IPPCCE Newsl.* 8, 5–26.
- Bloemendal, J., King, J.W., Hall, F.R., Doh, S.-J., 1992. Rock magnetism of Late Neogene and Pleistocene deep-sea sediments relationship to sediment source, diagenetic processes, and sediment lithology. *J. Geophys. Res.* 97 (b4), 4361–4375.
- Ceramicola, S., Rebesco, M., De Batist, M., Khlystov, O., 2002. Seismic evidence of small-scale lacustrine drifts in Lake Baikal (Russia). *Mar. Geophys. Res.* 22 (5–6), 445–464.
- Colman, S.M., Peck, J.A., Karabanov, E.B., Carter, S.J., Bradbury, J.P., King, J.W., Williams, D.F., 1995. Continental climate response to orbital forcing from biogenic silica records in Lake Baikal. *Nature* 378, 769–771.
- Day, R., Fuller, M., Schmidt, V.A., 1977. Hysteresis properties of titanomagnetites grain-size and compositional dependence. *Phys. Earth Planet. Inter.* 13, 260–267.
- Dearing, J.A., Boyle, J.F., Appleby, P.G., Mackay, A.W., Flower, R.J., 1998. Magnetic properties of recent sediments in Lake Baikal, Siberia. *J. Paleolimnol.* 20 (2), 163–173.
- Deike, R.G., Granina, L., Callender, E., McGee, J.J., 1997. Formation of ferric iron crusts in Quaternary sediments of Lake Baikal, Russia, and implications for paleoclimate. *Mar. Geol.* 139, 21–46.
- Dekkers, M.J., Passier, H.F., Schoonen, M.A.A., 2000. Magnetic properties of hydrothermally synthesized greigite (Fe<sub>3</sub>S<sub>4</sub>)-II: high- and low-temperature characteristics. *Geophys. J. Int.* 141 (3), 809–819.
- Demory, F., Nowaczyk, N.R., Witt, A., Oberhänsli, H., 2005. High-resolution magnetostratigraphy of late Quaternary sediments from Lake Baikal, Siberia: timing of intracontinental paleoclimatic responses. *Glob. Planet. Change* 46, 167–186 (this issue).
- Dunlop, D.J., 2002a. Theory and application of the day plot ( $M_{rs}/M_s$  versus  $H_{cr}/H_c$ ). 1: theoretical curves and tests using titanomagnetite data. *J. Geophys. Res.* 107 (B3), 4-1–4-22.
- Dunlop, D.J., 2002b. Theory and application of the day plot ( $M_{rs}/M_s$  versus  $H_{cr}/H_c$ ). 2: application to data for rocks, sediments, and soils. *J. Geophys. Res.* 107 (B3), 5-1–5-15.
- Fagel, N., Boski, T., Likhoshway, L., Oberhänsli, H., 2003. Late Quaternary clay mineral record in Central Lake Baikal (Academician Ridge, Siberia). *Palaeogeogr. Palaeoclimatol. Palaeoecol.* 193, 159–179.

- Florindo, F., P., R.A., Palmer, M.R., 2003. Magnetite dissolution in siliceous sediments. *Geochem. Geophys. Geosyst.* 4 (7), 1–13.
- Frank, U., Nowaczyk, N.R., Negendank, J.F.W., Melles, M., 2002. A paleomagnetic record from Lake Lama, northern Central Siberia. *Phys. Earth Planet. Inter.* 133 (1–4), 3–20.
- Grachev, M.A., Likhohway, E.V., Vorobieva, S.S., Khlystov, O.M., Bezrukova, E.V., Veinberg, E.V., Goldberg, E.L., Granina, L.Z., Kornakova, E.G., Lazo, F.I., Levina, O.V., Letunova, P.P., Otinov, P.V., Pirog, V.V., Fedotov, A.P., Yaskevitch, A.V., Bobrov, V.A., Sukhorukov, F.V., Rezhnikov, V.I., Fedorin, M.A., Zolotarev, K.V., Kravchinsky, V.A., 1997. Signals of the paleoclimates of upper Pleistocene in the sediments of Lake Baikal. *Geol. Geophys.* 38 (5), 957–980.
- Graham, J.W., 1966. Significance of magnetic anisotropy in Appalachian sedimentary rocks. *The Earth Beneath the Continents—A Volume of Geophysical Studies in Honor of Merle A. Tuve*. Geophysical Monograph American Geophysical Union, Washington, DC, United States, pp. 627–648.
- Granina, L., Muller, B., Wehrli, B., Martin, P., 2000. Oxygen, iron, and manganese at the sediment–water interface in Lake Baikal. *Terra Nostra* 9, 87–94.
- Granina, L., Müller, B., Wehrli, B., 2004. Origin and dynamics of Fe and Mn sedimentary layers in Lake Baikal. *Chem. Geol.* 205 (1–2), 55–72.
- Hilton, J., 1987. A simple model for the interpretation of magnetic records in lacustrine and ocean sediments. *Quat. Res.* 27 (2), 160–166.
- Hu, S., Appel, E., Hoffman, V., Schmahl, W., Wang, S., 1998. Gyromagnetic remanence acquired by greigite ( $\text{Fe}_3\text{S}_4$ ) during static three-axis alternating field demagnetisation. *Geophys. J. Int.* 134 (3), 831–842.
- Hu, S., Stephenson, A., Appel, E., 2002. A study of gyromagnetic magnetisation (GRM) and rotational remanent magnetisation (RRM) carried by greigite from lake sediments. *Geophys. J. Int.* 151 (2), 469–474.
- Hutchinson, D.R., Golmshtok, A.J., Zonenshain, L.P., Moore, T.C., Scholz, C.A., Klitgord, K.D., 1992. Depositional and tectonic framework of the rift basins of Lake Baikal from multichannel seismic data. *Geology* 20, 589–592.
- Jansen, J.H.F., Van der Gaast, S.J., Koster, B., Vaars, A.J., 1998. CORTEX, a shipboard XRF-scanner for element analyses in split sediment cores. *Mar. Geol.* 151 (1–4), 143–153.
- Kletetschka, G., Wasilewski, P.J., 2002. Grain size limit for SD hematite. *Phys. Earth Planet. Inter.* 129 (1–2), 173–179.
- Kravchinsky, V.A., Krainov, M.A., Evans, M.E., Peck, J.A., King, J.W., Kusmin, M.I., Sakai, H., Kawai, T., Williams, D.F., 2003. Magnetic record of Lake Baikal sediments chronological and paleoclimatic implication for the last 6.7 Myr. *Palaeogeogr. Palaeoclimatol. Palaeoecol.* 195, 281–298.
- Larson, A.C., Von Dreele, R.B., 1987. Generalized structure analysis system, Los Alamos National Laboratory Report: No. LA-UR-86-748.
- Liu, Q.B., Banerjee, S.K., Jackson, M.J., Zhu, R., Pan, Y., 2002. A new method in mineral magnetism for the separation of weak antiferromagnetic signal from a strong ferrimagnetic background. *Geophys. Res. Lett.* 29 (12), 6-1–6-4.
- Maher, B.A., Dennis, P.F., 2001. Evidence against dust-mediated control of glacial–interglacial changes in atmospheric  $\text{CO}_2$ . *Nature* 411 (6834), 176–180.
- Nowaczyk, N.R., Harwart, S., Melles, M., 2000. A rock magnetic record from Lama Lake, Taymyr Peninsula, northern Central Siberia. *J. Paleolimnol.* 23 (3), 227–241.
- Oberhänsli, H., 2000. Searching for climate proxies stored in Lake Baikal sediments: a few comments. *Terra Nostra* 9, 140–147.
- Oda, H., Nakamura, K., Ikehara, K., Nakano, T., Nishimura, M., Khlystov, O., 2002. Paleomagnetic record from Academician Ridge, Lake Baikal: a reversal excursion at the base of marine oxygen isotope stage 6. *Earth Planet. Sci. Lett.* 202 (1), 117–132.
- Oldfield, F., 1998. The rock magnetic identification of magnetic mineral and grain size assemblages. In: Walden, J., Oldfield, F., Smith, J. (Eds.), *Environment Magnetism, A Practical Guide*. Quaternary Research Association, pp. 98–112.
- Oldfield, F., Darnley, I., Yates, G., France, D.E., Hilton, J., 1992. Storage diagenesis versus sulphide authigenesis possible implications in environmental magnetism. *J. Paleolimnol.* 7 (3), 179–189.
- Peck, J.A., King, J.W., 1996. Magnetofossils in the sediments of lake Baikal, Siberia. *Earth Planet. Sci. Lett.* 140 (1–4), 159–172.
- Peck, J.A., King, J.W., Colman, S.M., Kravchinsky, V.A., 1994. A rock-magnetic record from Lake Baikal, Siberia: evidence for Late Quaternary climate change. *Earth Planet. Sci. Lett.* 122, 221–238.
- Piotrowska, N., Bluszcz, A., Demske, D., Granoszewski, W., Heumann, G., 2004. Extract-ion and AMS radiocarbon dating of pollen from Lake Baikal sediments. *Radiocarbon* 46 (1), 181–188.
- Prokopenko, A.A., Karabanov, E.B., Williams, D.F., Kusmin, M.I., Shackleton, N.J., Crowhurst, S.J., Peck, J.A., Gvozdkov, A.N., King, J.W., 2001. Biogenic silica record of the Lake Baikal response to climatic forcing during the Brunhes. *Quat. Res.* 55 (2), 123–132.
- Rees, A.I., 1965. The use of anisotropy of magnetic susceptibility in the estimation of sedimentary fabric. *Sedimentology* 4 (4), 257–271.
- Roberts, A.P., 1995. Magnetic properties of sedimentary greigite ( $\text{Fe}_3\text{S}_4$ ). *Earth Planet. Sci. Lett.* 134 (3–4), 227–236.
- Sakai, H., Nomura, S., Horii, M., Kashiwaya, K., Tanaka, A., Kawai, T., Kravchinsky, V., Peck, J., King, J., 2000. Paleomagnetic and rock-magnetic studies on Lake Baikal sediments—BDP96 borehole at Academician Ridge. In: Minoura, K. (Ed.), *Lake Baikal*. Elsevier Science, pp. 35–52.
- Shackleton, N.J., Berger, A., Peltier, W.R., 1990. An alternative astronomical calibration of the lower Pleistocene timescale based on ODP site 677. *Trans. R. Soc. Edinb. Earth Sci.* 81, 251–261.
- Sherman, S.I., Gladkov, A.S., 1999. Fractals in studies of faulting and seismicity in the Baikal rift zone. *Tectonophysics* 308 (1–2), 133–142.
- Smimov, A.V., Tarduno, J.A., 2000. Low-temperature magnetic properties of pelagic sediments (Ocean Drilling Program Site 805C): tracers of maghemitization and magnetic mineral reduction. *J. Geophys. Res., B: Solid-Earth* 105 (7), 16457–16471.

- Snowball, I.F., 1993. Geochemical control of magnetite dissolution in subarctic lake sediments and the implications for environmental magnetism. *J. Quat. Sci.* 8 (4), 339–346.
- Snowball, I.F., 1994. Bacterial magnetite and the magnetic properties of sediments in a Swedish lake. *Earth Planet. Sci. Lett.* 126 (1–3), 129–142.
- Snowball, I.F., Thompson, R., 1990. A stable chemical remanence in Holocene sediments. *J. Geophys. Res.* 95 (B4), 4471–4479.
- Stacey, F.D., Joplin, G., Lindsay, J., 1960. Magnetic anisotropy and fabrics of some foliated rocks from S. E. Australia. *Geofiz. Pura Appl.* 47, 30–40.
- Stephenson, A., 1980. A gyroremanent magnetisation in anisotropic magnetic material. *Nature* 284, 49–51.
- Stephenson, A., Snowball, I.F., 2001. A large gyromagnetic effect in greigite. *Geophys. J. Int.* 145 (2), 570–575.
- Thompson, R., Bloemendal, J., Dearing, J.A., Oldfield, F., Rumery, T.A., Stober, J.C., Turner, G.M., 1980. Environmental applications of magnetic measurements. *Science* 207, 481–486.
- Thouveny, N., de Beaulieu, J.-L., Bonifay, E., Creer, K.M., Guiot, J., Icole, M., Johnsen, S., Jouzel, J., Reille, M., Williams, T., Williamson, D., 1994. Climate variations in Europe over the past 140 kyr deduced from rock magnetism. *Nature* 371, 503–506.
- Verosub, K.L., 1977. Depositional and postdepositional processes in the magnetization of sediments. *Rev. Geophys. Space Phys.* 15 (2), 129–143.
- Watanabe, T., Naraoka, H., Nishimura, M., Kawai, T., 1977. Biological and environmental changes in Lake Baikal during the late Quaternary inferred from carbon, nitrogen and sulfur isotopes. *Earth Planet. Sci. Lett.* 222 (1), 285–299.
- Weiss, R.F., Carmack, E.C., Koropalov, V.M., 1991. Deep-water renewal and biological production in Lake Baikal. *Nature* 349, 665–669.
- Williamson, D., Jelinowska, A., Kissel, C., Tucholka, P., Gibert, E., Gasse, F., Massault, M., Taieb, M., Van Campo, E., Wieckowski, K., 1998. Mineral-magnetic proxies of erosion/oxidation cycles in tropical maar-lake sediments (Lake Tritrivakely, Madagascar) paleoenvironmental implications. *Earth Planet. Sci. Lett.* 155 (3–4), 205–219.